



Research Paper

ANALYSIS OF METALLIC AND COMPOSITE TAIL ROTOR DRIVE SHAFT FOR BALLISTIC IMPACT

Hemanth Kumar C^{1*} and Swamy R P²

*Corresponding Author: Hemanth Kumar C, ✉ hemanthkumar.sh17@gmail.com

Rotorcraft, especially in military applications, can experience damage during regular operation. One particular type of damage that is of relevance to the driveline system is the introduction of holes into the shaft. Holes can arise from ballistic damage to the shaft, and characterizing the effects that holes have on stiffness, strength, and stability of the driveline system is of major interest to the designer. In this work the ballistic damage tolerance capability of aluminum and composite drive shaft segment with and without damage at different locations are carried out for various boundary conditions to determine strength, stiffness using conventional stress analysis and FEA package, Ansys.

Keywords: Rotorcraft, Ballistic damage, Drive shaft, FEA, Ansys

INTRODUCTION

Rapid technological advances in engineering brought the scientists and engineers to a point, where they became limited by the capabilities of traditional materials. With the limits of the technology pushed, the materials failed to answer the requirements of the designers or manufacturers. Researchers in materials technology are constantly looking for solutions to provide stronger, durable materials which will answer the needs of their fellow engineers. Composite materials are one of the most favored solutions to this problem in the field.

Replacement of steel shaft by composite shaft is a novelty all over the world. Composite materials have interesting properties such as high strength to weight ratio, compared to metals, which make them very attractive for rotating systems. The composite-material shafts have been sought as new potential candidates for replacement of the conventional metallic shafts in many application areas such as: drive shafts for helicopters, centrifugal separators, and cylindrical tubes for the automotive and marine industries. Replacing metallic shafts by composite shafts reduces the overall system weight by 30%; moreover,

¹ Department of Mechanical Engineering, Sai Vidya Institute of Technology, Bangalore, India.

² Department of Studies in Mechanical Engineering, UBBDT College of Engineering, Davangere, Karnataka, India.

the composite shaft is twice as stiff as a comparable aluminum shaft.

The advanced composite materials such as Graphite, Carbon and Glass with suitable resins are widely used because of their high specific strength (strength/density) and high specific modulus (modulus/density). Advanced composite materials seem ideally suited for long, power driver shaft (propeller shaft) applications. Their elastic properties can be tailored to increase the torque they can carry as well as the rotational speed at which they operate. The drive shafts are used in automotive, aircraft and aerospace applications. They also provide designers with the possibility of obtaining predetermined behaviors, in terms of position of critical speeds, by changing the arrangement of the different composite layers: orientation and number of plies. On the other hand, these materials have relatively high-damping characteristics. For a rotor made with composite materials, internal damping is much more significant compared with those associated with a metal rotor.

LITERATURE REVIEW

In recent years research is going on to replace the conventional steel drive shaft with a high specific strength and high specific modulus composite drive shaft for an automotive and aerospace application to evaluate torsional properties of composite shafts over conventional steel shaft.

Abu Talib *et al.* (2010) designed composite drive shafts incorporating carbon and glass fibers within an epoxy matrix for a configuration of one layer of carbon-epoxy and three layers of glass-epoxy with 0°, 45° and 90°.

Mutasher (2009) has investigated the effect of stacking sequence angle on static and dynamic characteristic of the hybrid aluminum/composite drive shaft.

Ercan Sevkat and Hikmet Tumer (2013) presented an experimental and numerical study to investigate residual torsional properties of composite shafts subjected to impact loadings.

Mahmood Shokrieh *et al.* (2013) have performed a FEM analysis to predict torsional stability of carbon/epoxy composite shafts with different ply sequences and the material properties to study the effects of boundary conditions, fiber orientation and stacking sequence on the mechanical behavior.

Khoshravan and Paykani (2012) presented a design method and a vibration analysis of a carbon/epoxy composite drive shaft.

OBJECTIVE

Although composites offer many unique advantages over traditional materials, they remain sensitive to impact loading. When a composite material is subjected to low-velocity or ballistic impact, delaminations, matrix cracking and fiber breakage may result. This, in turn, leads to a reduction in the component's residual strength. Repair of such damaged parts is often difficult and time consuming. Thus, it would be highly beneficial to develop means of improving damage tolerance so that repair becomes unnecessary.

Rotorcraft, especially in military applications, can experience damage during regular operation. One particular type of damage that is of relevance to the driveline system is the introduction of holes into the shaft.

Holes can arise from ballistic damage to the shaft, and characterizing the effects that holes have on stiffness, strength, and stability of the driveline system is of major interest to the designer.

The objective of this work is to study the ballistic damage tolerance capability of metallic and composite shaft segment with respect to strength, stiffness using conventional stress analysis and FEM package.

METHODOLOGY

This work deals with conventional stress analysis and FEA of tail drive metal shaft. It also involves FEA of metallic and composite shaft segment with and without damage at different location for various boundary conditions and comparison of FEA results of metallic and composite shaft.

Table 1: Material Properties of Aluminium Tail Rotor Drive Shaft	
Material	Al. Alloy Tube 2618 A (AIR 9049) T851
Young's Modulus, E	74000 N/mm ²
Poisson's Ratio, ~	0.33
Modulus of Rigidity, G	28462 N/mm ²
Ultimate Shear Stress, ‡ _{ULT}	254 N/mm ²

Table 2: Dimensions of Tail Rotor Drive Shaft	
Outer diameter, d _o	63 mm
Inside diameter, d _i	59.8 mm
Wall thickness, t	1.6 mm
Length of the shaft, L	1130 mm

STRESS ANALYSIS

1. Torsional Shear Stress (‡_t) = (T/J) x r ... (1)

T = Torque in N-m

J = Polar moment of inertia, mm⁴

r = Outer radius of tube, mm

a. For power = 250 kw, T = 590 Nm

‡_t = 63.85 N/mm²

2. Angle of Twist, (q)

q = T.L/(G.J) x (180/f) deg ... (2)

a. For power = 250 kw, T = 590 Nm

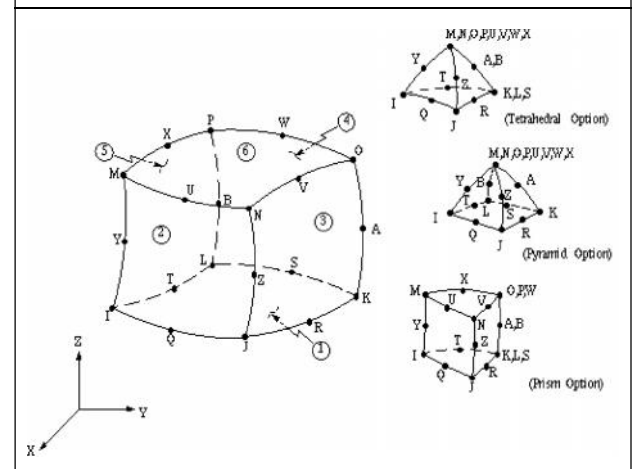
q = 4.62 deg.

FINITE ELEMENT ANALYSIS

Solid-95 Element

This element is a higher order version of the 3-D 8-node solid element (SOLID45). It can tolerate irregular shapes without as much loss of accuracy. SOLID95 elements have compatible displacement shapes and are well suited to model curved boundaries. The element is defined by 20 nodes having three degrees of freedom per node: translations in the nodal x, y, and z directions. The element may have any spatial orientation. The element has plasticity, creep, stress stiffening, large

Figure 1: Solid95 3-D 20-Node Structural Solid



deflection, and large strain capabilities. The geometry, node locations, and the coordinate system for this element are shown in Figure 1.

Besides the nodes, the element input data also includes the orthotropic material properties.

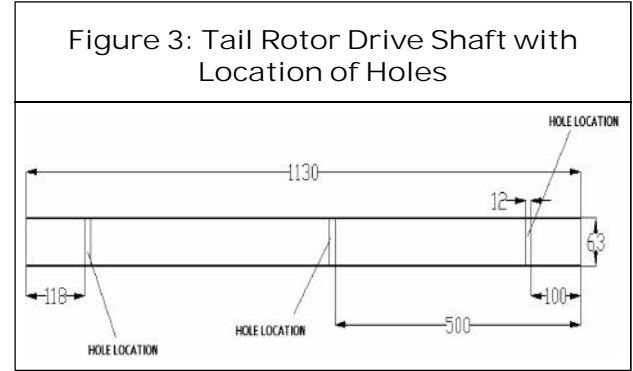
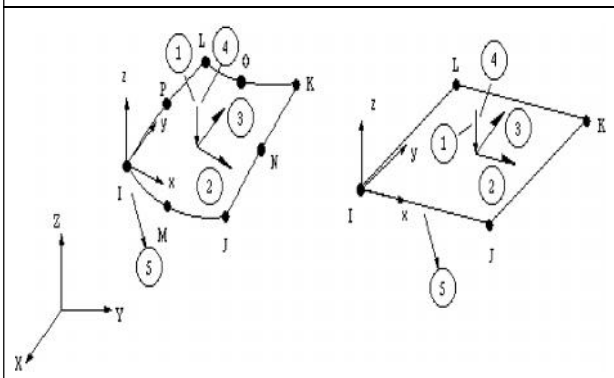
Surface Element

Surface effect elements have no physical properties. These elements are mainly used for loading purposes only. They are overlaid like a “skin” on structural (and thermal) element faces. SURF154 may be used for various load and surface effect applications. It may be overlaid onto an area face of any 3-D element. The element is applicable to three-dimensional

structural analyses. Various loads and surface effects may exist simultaneously.

Figure 3 shows the dimensional details of the tail rotor drive shaft with location of holes.

Figure 2: SURF154 3-D Structural Surface Effect Element



Figures 4 and 5 shows the finite element model for aluminum and composite shaft.

Table 3: Material Properties of E-Glass/ Epoxy Drive Shaft

Parameter	E-Glass/Epoxy
E_x (GPa)	40.3
E_y (GPa)	6.21
E_z (GPa)	40.3
$\mu_{xy=yz=zx}$	0.2
G_{xy} (GPa)	3.07
G_{yz} (GPa)	1.55
G_{xz} (GPa)	2.39
Density (Kg/m ³)	1910

Figure 4: FEM Model for Aluminum Shaft

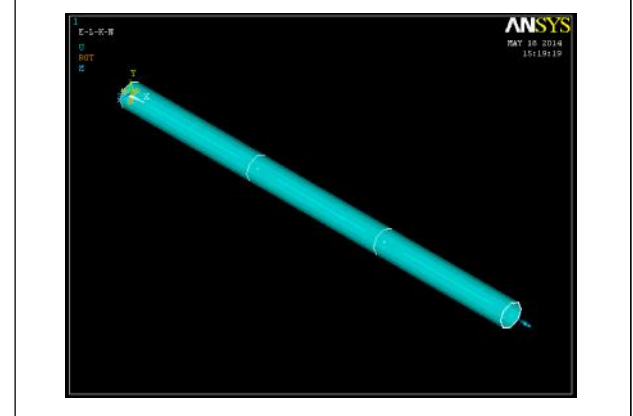


Figure 5: FEM Model for Composite Shaft

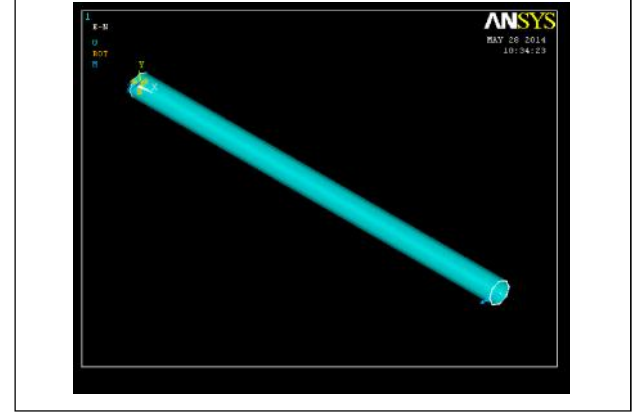


Figure 6: Shaft Model with Hole at Both Edges

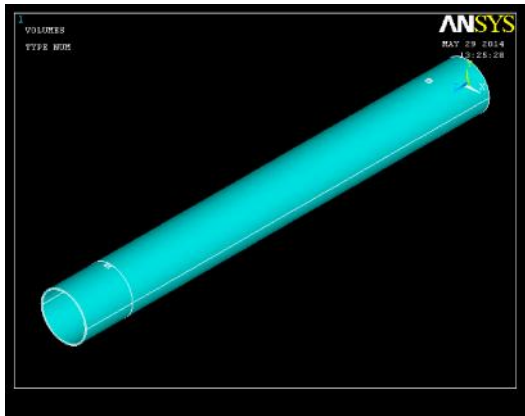


Figure 7: Shaft Model with Hole at Three Points

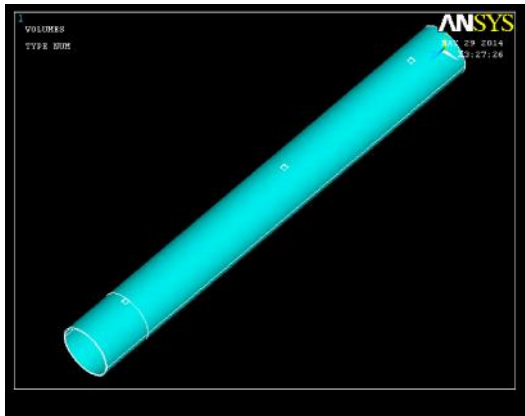


Figure 8: Finite Element Meshed Model with Torque Application

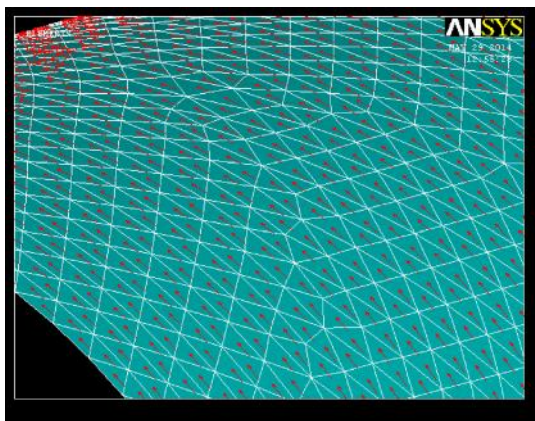


Figure 6 shows Finite element model for aluminum and composite shaft with hole at both edges and Figure 7 shows finite element model for aluminum and composite shaft with hole at three points.

RESULTS AND DISCUSSION

Figures 9 and 10 shows angel of twist and torsional shear stress for aluminum shaft.

Figure 9: Angle of Twist of Aluminium Drive Shaft

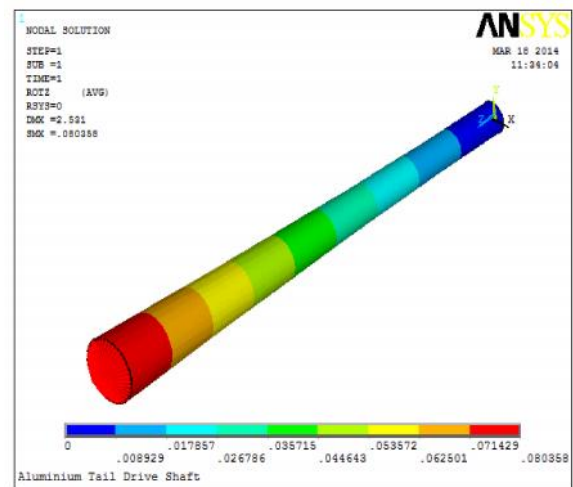
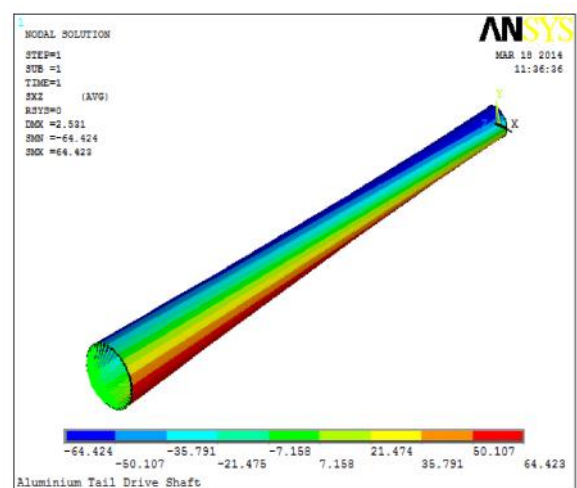


Figure 10: Torsional Shear Stress of Aluminium Shaft



Figures 11 and 12 shows Displacement vector sum and von Mises stress of aluminum shaft with the hole at both edges.

Figure 11: Displacement Vector Sum of Aluminium Shaft with Hole at Both Edges

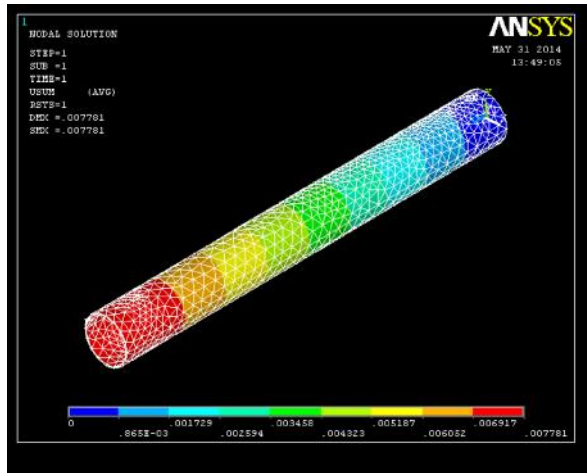
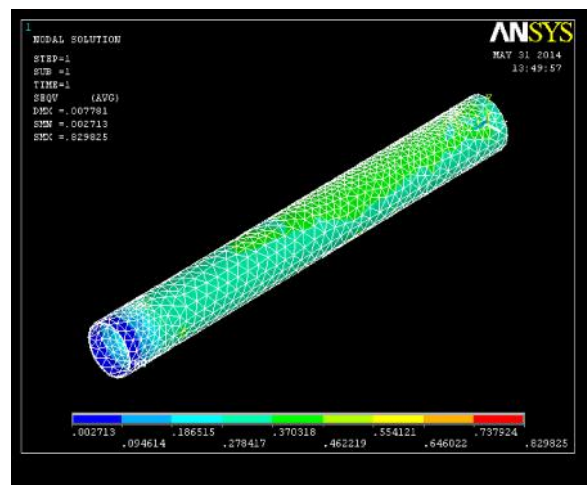


Figure 12: Von Mises Stress for Aluminium Shaft at Both Edges of a Hole



Figures 13 and 14 shows Displacement vector sum and von Mises stress of aluminum shaft with the hole at three points.

Figures 15 and 16 shows Rotational vector sum and Von Mises stress of composite shaft with the hole at two edges.

Figure 13: Displacement Vector Sum of Aluminium Shaft with Hole at Three Locations

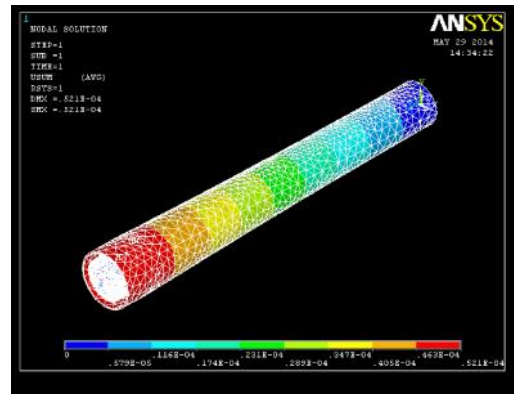


Figure 14: Von Mises Stress for Aluminium Shaft at the Hole at Three Locations

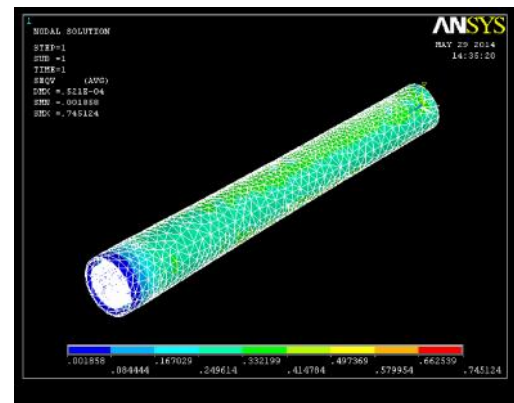


Figure 15: Rotational Vector Sum of Composite Shaft at the Hole at Both Edges

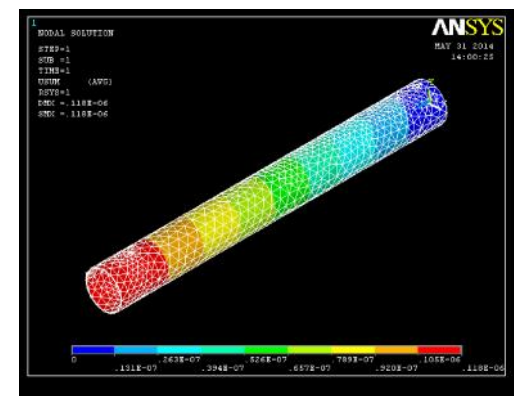


Figure 16: Von Mises Stress for Composite Shaft at Both Edges of a Hole

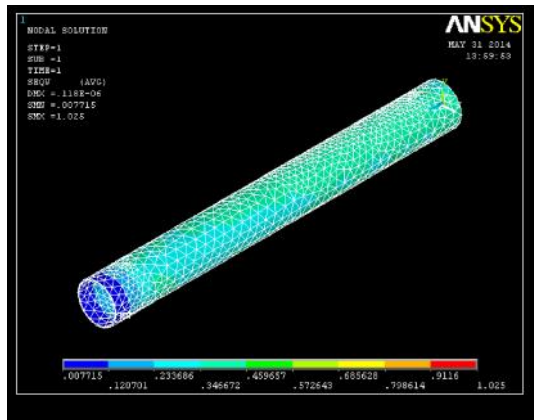


Figure 17: Rotational Vector Sum of Composite Shaft with Hole at Three Locations

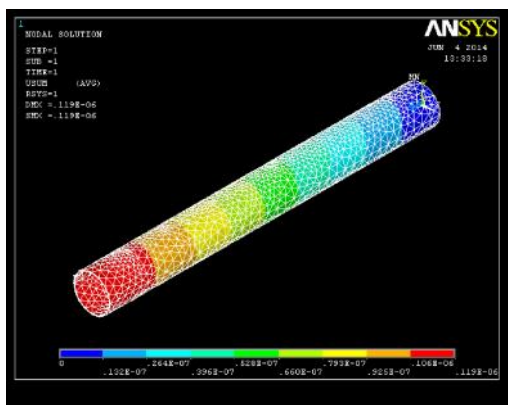
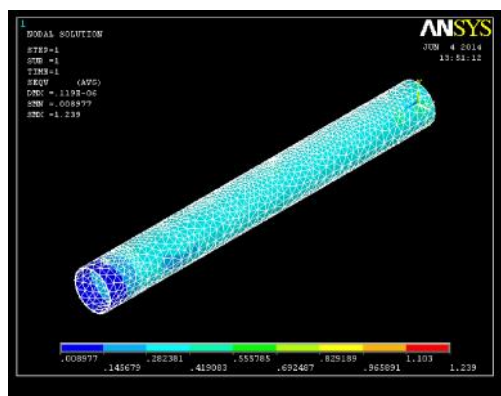


Figure 18: Von Mises Stress for Composite Shaft at the Hole at Three Locations



Figures 17 and 18 shows Rotational vector sum and Von Mises stress of composite shaft with the hole at three locations.

CONCLUSION

The variation of stresses and deformation of aluminum and E-Glass/Epoxy composite shaft along the thickness were within the allowable limit. Maximum displacement was observed at load application edge. Maximum stress was observed at the vicinity of holes. Also there is no impact of the holes even though the shaft segment is at three locations and the helicopter will successfully land without any obstruction after the damage. Composite shafts can also be used as an alternate since it satisfies damage tolerance criteria and with many advantages like considerable amount of weight reduction when compared to conventional metallic shaft.

REFERENCES

1. Abu Talib AR, Aidy Ali, Mohamed A Badie, Nur Azida Che Lah and Golestaneh A F (2010), "Developing a Hybrid, Carbon/ Glass Fiber-Reinforced, Epoxy Composite Automotive Drive Shaft", *Materials and Design, Elsevier Science*.
2. *Composite Materials Handbook*, Mein Schwartz, McGraw Hill Book Company.
3. Ercan Sevkati and Hikmet Tumer (2013), "Residual Torsional Properties of Composite Shafts Subjected to Impact Loadings", *Materials and Design, Elsevier Science*.
4. Khoshravan M R and Paykani A (2012), "Design of a Composite Drive Shaft", *Journal of Applied Research*, Vol. 10, December 6, pp. 826-834.

5. Mahmood M Shokrieh, Akbar Hasani and Larry B Lessard (2013), "Shear Buckling of a Composite Drive Shaft Under Torsion", *Composite Structures, Elsevier Science*.
6. Mutasher S A (2009), "Prediction of the Torsional Strength of the Hybrid Aluminum/Composite Drive Shaft", *Materials and Design, Elsevier Science*.